[1] Nihon University, [2] Research Institute of Salt and Sea Water Science, [3] Chiba Institute of Technology
M. Matsumoto[1*], K. Masaoka[2], Y. Tsuchiya[1], Y. Wada[1], T. Hiaki[1], K. Onoe[3]

Enhanced $CaMg(CO_3)_2$ Production by CO_2 Microbubble Injection into Concentrated brine

Salt Production

Keywords: Microbubbles, Reactive crystallization, Concentrated brine, Dolomite, Mg/Ca ratio, fine particles

Abstract

In order to build a utilization system of seawater resources based on the desalination and salt production process and to prevent scaling in reverse osmosis and electrodialysis units, a recovery and upgrading method for calcium (Ca) and magnesium (Mg) from the concentrated brine discharge from salt manufacture in Japan was investigated. The reactive crystallization technique of carbonate using carbon dioxide (CO_2) bubbling is effective for a separation/recovery method of the dissolved Ca^{2+} and Mg^{2+} in the concentrated brine, because the solubility of carbonate is lower than the solubility of hydroxide in the solution at a pH range below 8.0. Especially, dolomite ($CaMg(CO_3)_2$), which is double salt of calcium carbonate and magnesium carbonate, has numerous applications as the manufacture of refractories, as neutralizer of soil acidity in agriculture, as mineral supplement for food and drug, etc.. $CaMg(CO_3)_2$ has crystal structure derived from that of calcite by ordered replacement Ca^{2+} in calcite by Mg^{2+}. To improve the functionality of crystal for the better $CaMg(CO_3)_2$ utilization, it is essential to gain access to the Mg/Ca ratio of 1.0 and to reduce the particle size in the crystallization process. Generally, high concentrations of Ca^{2+}, Mg^{2+} and CO_3^{2-} are necessary for the production of $CaMg(CO_3)_2$ with a Mg/Ca ratio of 1.0, because the Mg/Ca ratio increases with increasing the supersolubility product in the bulk solution.

In this study, the micron-scale bubble formation technique that enables the generation of regions with a higher ion concentration around the minute gas-liquid interfaces was applied to the reactive crystallization of $CaMg(CO_3)_2$. In the regions near the minute gas-liquid interfaces, Ca^{2+} and Mg^{2+} accumulate because of the negative electric charge on the microbubble surface, and the concentration of CO_3^{2-} increases because of the acceleration of CO_2 mass transfer caused by minimizing the bubble diameter; hence, the fine particles of $CaMg(CO_3)_2$ with a high Mg/Ca ratio can be expected to crystallize.

At a reaction temperature of 298 K and reaction pH of 6.8, CO_2 bubbles with an average diameter (d_{bbl}) of 40 - 2000 μm were continuously supplied to the concentrated brine coming from salt manufacture discharge and $CaMg(CO_3)_2$ was crystallized within the reaction time (t_r) of 120 min. Microbubbles with a d_{bbl} of 40 μm were generated using a self-supporting bubble generator by the shear of the impeller and a negative pressure owing to high-rotation. For comparison, the bubbles with a d_{bbl} of 200, 300, 800 or 2000 μm were obtained using a dispersing-type generator. Consequently, minimizing the bubble formation accelerated remarkably the crystallization of $CaMg(CO_3)_2$ fine particles with an average size of about 2.0 μm and decreased t_r necessary for the achievement of Mg/Ca ratio of 1.0.

E-mail address: matsumoto.masakazu@nihon-u.ac.jp Phone: +81-47-474-2850

[1] Nihon University, [2] Research Institute of Salt and Sea Water Science, [3] Chiba Institute of Technology
M. Matsumoto[1*], K. Masaoka[2], Y. Tsuchiya[1], Y. Wada[1], T. Hiaki[1], K. Onoe[3]

Introduction

In this study, the microbubble technique was applied to the reactive crystallization of carbonate from concentrated brine coming from salt manufacture discharge. In Japan, in order to build up a utilization system of seawater resources based on salt production process, a recovery and upgrading method for calcium (Ca) and magnesium (Mg) from the discharge concentrated brine of salt manufactory is desired. From the viewpoint of solubility of salts, the synthesis of carbonate by reactive crystallization between the dissolved Ca^{2+} and Mg^{2+} in the concentrated brine and carbon dioxide (CO_2) can be considered an effective separation/recovery method because the solubility of carbonate is lower than the solubility of hydroxide in the solution at a pH range below 8.0 [1,2]. In particular, $CaMg(CO_3)_2$ is double salt of calcium carbonate and magnesium carbonate and has numerous applications as the manufacture of refractories, as neutralizer of soil acidity in agriculture, as mineral supplement for food and drug, etc. [3-7]. $CaMg(CO_3)_2$ has crystal structure derived from that of calcite by ordered replacement Ca^{2+} in calcite by Mg^{2+} [6,7]. To improve the functionality of crystal for the better $CaMg(CO_3)_2$ utilization, it is necessary to achieve the Mg/Ca ratio of 1.0 and to reduce the particle size in the crystallization operation. Although extensive research on the synthesis of $CaMg(CO_3)_2$ with the Mg/Ca ratio of 1.0 at high temperature and pressure has been carried out [8-14], the methods that produce $CaMg(CO_3)_2$ by reactive crystallization under normal temperature and pressure are not fully identified. Generally, high concentrations of Ca^{2+}, Mg^{2+} and CO_3^{2-} are necessary for the synthesis of $CaMg(CO_3)_2$ with a Mg/Ca ratio of 1.0, as the Mg/Ca ratio increases with an increase in the supersaturation of the bulk solution [15].

With the development of the micron-scale bubble formation technique to obtain bubbles whose size is < 50 μm, considerable attention has been paid to the application of the so-called “microbubbles” [16]. Minimizing bubble size causes the gas-liquid interface area, average residence time and inner pressure of bubbles to increase, and consequently the mass transfer and reactive absorption is accelerated. Additionally, the effects of specific interactions at the gas-liquid interface caused by electrification of microbubbles become available [17,18]. Accordingly, by increasing the residence time of microbubbles with surface potential in the liquid phase for a long period time, a quasi-homogeneous gas-liquid system can be obtained and unique mass-transfer patterns and reaction phenomena are expected to occur. In this study, the microbubble formation technique that enables the generation of regions with a greater ion concentration near the minute gas-liquid interfaces was applied to the reactive crystallization of $CaMg(CO_3)_2$ under the atmospheric temperature and pressure. When the microbubbles that changed the feed source into the CO_2 gas are introduced into the reactive crystallization of $CaMg(CO_3)_2$ in this work, Ca^{2+} and Mg^{2+} accumulate because of the negative charge on the microbubble surface, and the CO_3^{2-} concentration becomes higher due to the acceleration of the CO_2 mass transfer caused by minimizing the bubble diameter. Hence, the gas-liquid interfaces of the microbubbles can be utilized as novel reactive crystallization fields, where the generation of crystal nuclei is faster and the fine particles of $CaMg(CO_3)_2$ with a high Mg/Ca ratio is crystallized [19,20]. In this paper, the effects of minimizing the bubble diameter on the reactive crystallization of $CaMg(CO_3)_2$ was examined. Additionally, we report also the effects of the CO_2 flow rate during reactive crystallization with CO_2 microbubble injection.

E-mail address: matsumoto.masakazu@nihon-u.ac.jp Phone: +81-47-474-2850

2. Experimental

2.1 Concentrated brine

The concentrated brine was coming from salt manufacture discharge in Japan. NaCl is manufactured by evaporative crystallization after concentrating seawater through an electric dialysis membrane, and the concentrated brine that removed K^+ by cooling crystallization was obtained concurrently with sodium chloride. The concentrations of $MgCl_2$, NaCl and $CaCl_2$ as the major components of the concentrated brine are 1.8, 1.2, and 0.5 mol/*l*, respectively [19,20].

2.2 Experimental apparatus

The semi-batch crystallization apparatus comprises a gas flow controller (FCC-3000-G1, KOFLOC Co.), a pH/EC meter (WM-50EG, TOA Electronics Co.), a self-supporting type bubble generator (Tech Ind.), a dispersing-type bubble generator (hole size of dispersing plate: 65 - 300 μm), a crystallization vessel, and a thermostat bath [17]. Microbubbles with an average diameter (d_{bbl}) of 40 μm were generated using a self-supporting type generator by the shear of the impeller and a negative pressure due to high-rotation [20], with the rotation rate maintained at 1500 min^{-1} and the CO_2 flow rate (F_{CO2}) controlled in the range between 1.49 and 23.8 mmol/(*l*·min). The bubbles with a d_{bbl} of 200, 300, 800 or 2000 μm were obtained for comparison using a dispersing-type generator at F_{CO2} of 5.96 - 23.8 mmol/(*l*·min), and the concentrated brine in a crystallizer was agitated using a propeller-type mixer with four blades at 800 min^{-1}. The d_{bbl} was determined from the bubble size distribution measured by a laser particle size analyzer (LA-920, Horiba, Ltd., Japan) and by a visualization method using the digital microscope (VH-5000, Keyence, Co., Japan).

2.3 Experimental procedure

CO_2 bubbles with d_{bbl} of 40, 200, 300, 800 or 2000 μm were continuously supplied to 300 mL of the concentrated brine, and $CaMg(CO_3)_2$ was crystallized in a crystallization vessel. The reaction temperature (T_r) was kept constant at 293 K using a thermostated bath, and the reaction time (t_r) was controlled within 120 min. The solution pH during crystallization was maintained constant at 6.8 by adding 4.0 mol/*l*-NaOH aqueous solution. After the crystallization progressed for a specified length of time, the suspension was filtered and the reaction products were washed with deionized water and then dried at 373 K in a dryer. The reaction products were identified by X-ray diffraction with Cu-K_α radiation. Measurement parameters were: acceleration voltage: 40 kV; filament current: 200 mA; counting time: 412 s; goniometer settings: 5.0°–60° 2θ; step size: 0.02° 2θ. The selectivity of solid products was determined by the peak area ratio from XRD, and the Mg/Ca ratio of $CaMg(CO_3)_2$ was estimated from the amount of peak shift from calcite (2θ = 29.4°) to $CaMg(CO_3)_2$ (2θ = 30.7°) [22-25]. The morphology and average size of the crystallized particles were observed using a scanning electron microscope (SEM, JSM-6300: Joel, Japan).

3. Experimental results and Discussion

3.1 Effects of minimization bubble diameter on reactive crystallization of $CaMg(CO_3)_2$ fine particles

In order to clarify the influence of minimizing the bubble diameter on the produced weight, Mg/Ca ratio, and particle size of $CaMg(CO_3)_2$, the reactive crystallization using CO_2 bubbles at a

E-mail address: matsumoto.masakazu@nihon-u.ac.jp Phone: +81-47-474-2850

[1] Nihon University, [2] Research Institute of Salt and Sea Water Science, [3] Chiba Institute of Technology
M. Matsumoto[1*], K. Masaoka[2], Y. Tsuchiya[1], Y. Wada[1], T. Hiaki[1], K. Onoe[3]

d_{bbl} of 40 - 2000 μm was performed. **Fig. 1** shows the time changes in the XRD pattern of the solid products, when CO_2 bubbles with d_{bbl} values of 40 and 2000 μm were supplied to the concentrated brine at F_{CO2} of 11.9 mmol/(l·min).

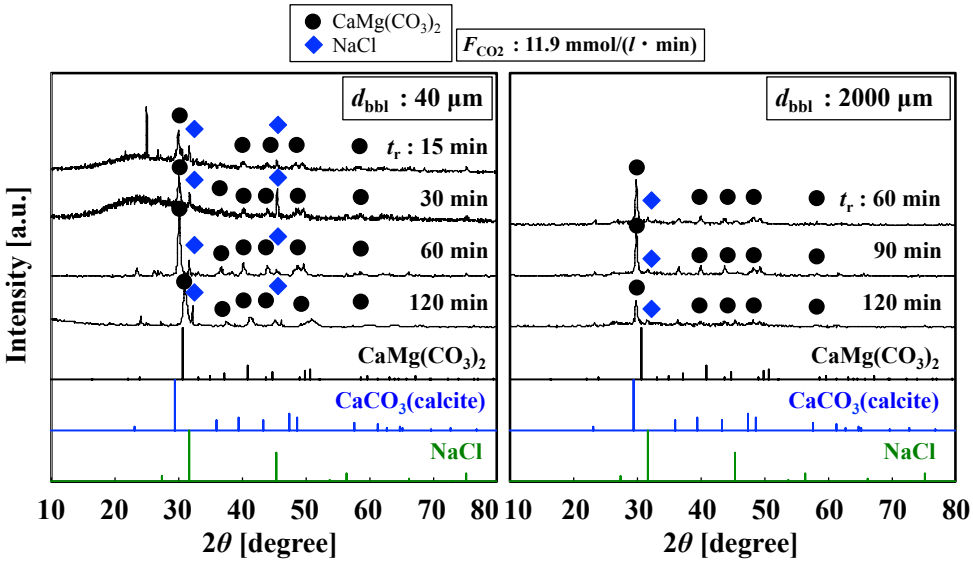

Fig. 1 Time changes in the XRD pattern of the solid products

The XRD patterns of $CaMg(CO_3)_2$ and NaCl were obtained for both values of d_{bbl}. The production of NaCl is because of the increase in Na^+ concentration by adding NaOH aqueous solution into the concentrated brine that is the saturated solution of NaCl and KCl. At a d_{bbl} of 40 μm, the XRD peak of calcite (2θ = 29.4°) shifted to $CaMg(CO_3)_2$ (2θ = 30.7°) with an increase in t_r. **Fig. 2** shows the time changes in the produced weight (W_i, i = $CaMg(CO_3)_2$, NaCl) and Mg/Ca ratio of $CaMg(CO_3)_2$ when F_{CO2} was set at 11.9 mmol/(l·min). At all d_{bbl} values the dominant products were $CaMg(CO_3)_2$ in which NaCl slightly contained. The induction period for nucleation, that is, the time between the initiation of CO_2 bubble supply and the formation of crystal nuclei, showed a tendency to reduce with a decrease in d_{bbl}. Furthermore, $W_{CaMg(CO3)2}$ increased remarkably with decreasing d_{bbl} in either t_r and $W_{CaMg(CO3)2}$ at d_{bbl} of 800, 300, 200 and 40 μm were 3.8, 5.3, 4.8 and 7.5 times greater than that of 2000 μm, respectively. Moreover, at a d_{bbl} of 2000 μm, the Mg/Ca ratio of $CaMg(CO_3)_2$ remained almost constant at 0.20. When d_{bbl} decreased to 40 μm, the Mg/Ca ratio increased linearly with t_r and was 0.86 at t_r of 120 min. The above results are observed probably because of the acceleration of CO_2 absorption and the electrification of the microbubble surface caused by minimization of the bubble diameter. So as to investigate the effects of the existence of $CaCl_2$ or $MgCl_2$ on the electrification of the microbubbles, the zeta potential around the gas-liquid interface was measured when

E-mail address: matsumoto.masakazu@nihon-u.ac.jp Phone: +81-47-474-2850

[1] Nihon University, [2] Research Institute of Salt and Sea Water Science, [3] Chiba Institute of Technology
M. Matsumoto[1*], K. Masaoka[2], Y. Tsuchiya[1], Y. Wada[1], T. Hiaki[1], K. Onoe[3]

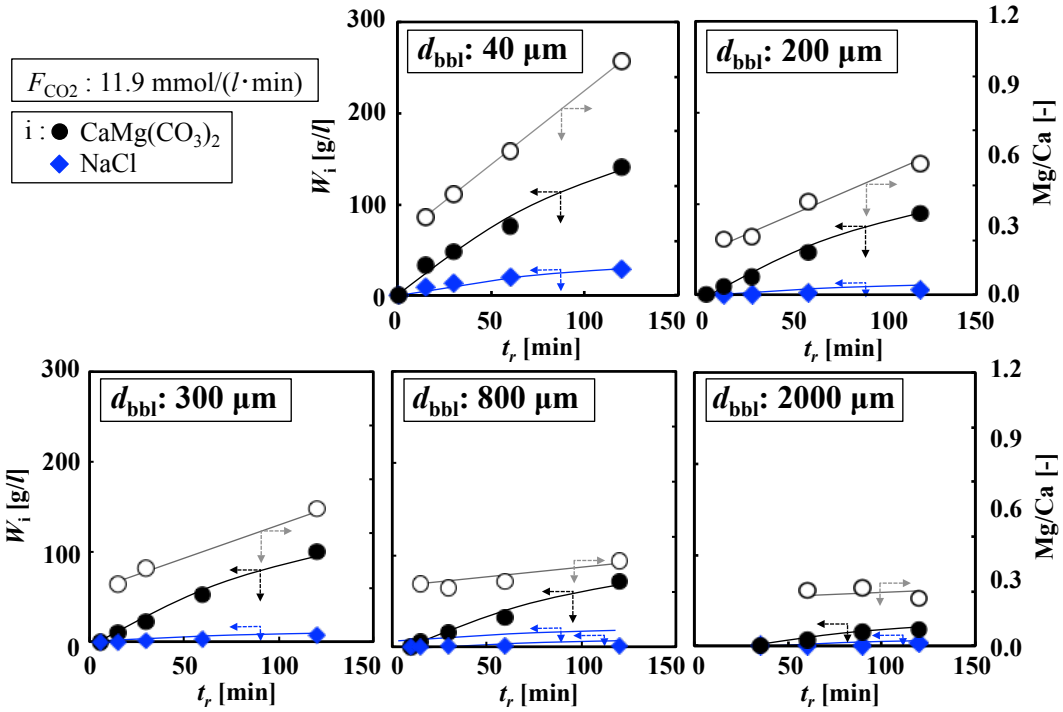

Fig. 2 Time changes in the produced weight (W_i, i = $CaMg(CO_3)_2$, NaCl) and Mg/Ca ratio of $CaMg(CO_3)_2$

microbubbles were supplied to distilled water, a 0.1 mol/*l*-$CaCl_2$, or a 0.1 mol/*l* -$MgCl_2$ aqueous solution [19,20]. The results showed that the zeta potential of microbubbles with a d_{bbl} of 10 - 30 μm ranged from -50 to -100 mV in distilled water and approached 0 mV by adding $MgCl_2$ or $CaCl_2$. These findings probably indicated that Mg^{2+} and Ca^{2+} concentrations increased locally in the boundary area of the gas-liquid interfaces of the microbubbles. Hence, $CaMg(CO_3)_2$ nucleation occurs easily at the minute gas-liquid interfaces, where the supersaturation is large locally, and $CaMg(CO_3)_2$ with a high Mg/Ca ratio was crystallized.

Fig. 3 shows SEM observation of the crystallized $CaMg(CO_3)_2$ when CO_2 bubbles with d_{bbl} in the range of 40 - 2000 μm were continuously supplied to the concentrated brine at t_r of 120 min.

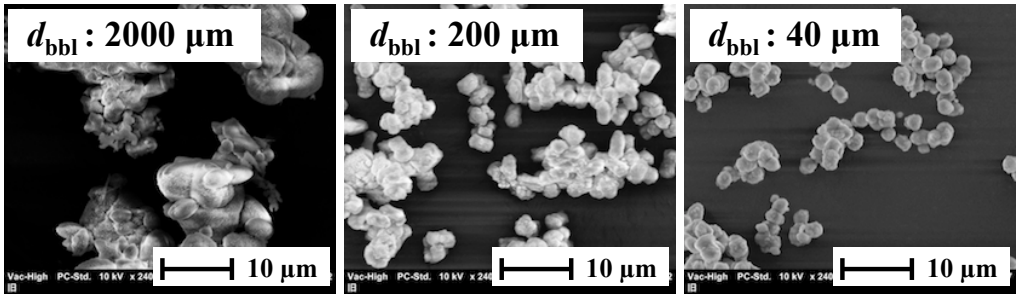

Fig. 3 Comparison of SEM observation of the crystallized $CaMg(CO_3)_2$

At a d_{bbl} of 40 μm, the spherical $CaMg(CO_3)_2$ particles with an average size of about 2 μm were observed, whereas the agglomerated particles with a size of almost 20 μm were obtained at d_{bbl} of 2000 μm. Kubota *et al*. [26] examined the relationship between supersaturation and nucleation and the growth rate of barium carbonate and reported that if the nucleation rate is relatively

E-mail address: matsumoto.masakazu@nihon-u.ac.jp Phone: +81-47-474-2850

suppressed in comparison with the crystal growth, the average particle size must be larger. Therefore, the minimized bubble diameter resulted in the micronization of the $CaMg(CO_3)_2$ particles because of nucleation acceleration caused by increasing local high supersaturation at the minute gas-liquid interfaces.

3.2 Relationship between CO_2 flow rate and Mg/Ca ratio or induction time for nucleation

With the aim to increase the effects of minute gas-liquid interfaces where the crystal nucleation progresses predominantly because of local increase in the concentrations of Ca^{2+}, Mg^{2+}, and CO_3^{2-}, the reactive crystallization of $CaMg(CO_3)_2$ using CO_2 microbubbles with a d_{bbl} of 40 μm was carried out by various F_{CO2} values between 1.49 and 23.8 mmol/(l·min) within t_r of 60 min at a constant T_r of 298 K. The results obtained from the time changes in W_i at various F_{CO2} values showed that at the smallest F_{CO2} of 1.49 mmol/(L·min) the crystal nucleation was not observed within t_r of 30 min. Therefore, the Mg/Ca ratio and W_i at a t_r of 60 min and the induction time for nucleation (t_{ind}) were plotted against F_{CO2} as shown in **Fig. 4**.

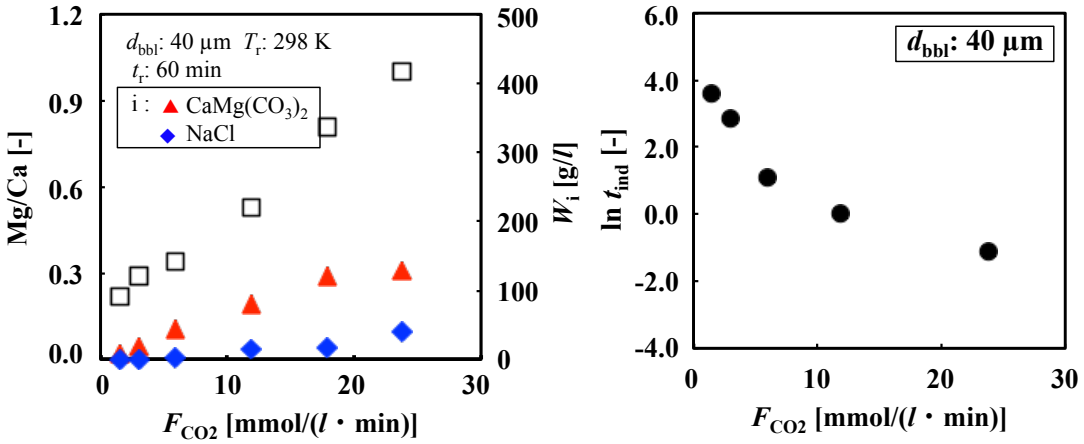

Fig.4 Relation between F_{CO2} and Mg/Ca ratio, W_i , and t_{ind}

$W_{dolomite}$ and W_{NaCl} increased as F_{CO2} increased. The Mg/Ca ratio increased linearly with increasing F_{CO2}, and the Mg/Ca ratio reached 1.0 when F_{CO2} was set at 23.8 mmol/(L·min). Moreover, t_{ind} had a tendency to decrease when F_{CO2} was increased. The effects of the concentration of Na_2CO_3 aqueous solution on the Mg/Ca ratio of $CaMg(CO_3)_2$ when the Na_2CO_3 solution was continuously added into the dissolved Ca^{2+} and Mg^{2+} solution were reported by Oomori *et al*. [15] and Fujimura *et al*. [27]. In their studies, a high concentration of Na_2CO_3 was more appropriate for the generation of $CaMg(CO_3)_2$ with a high Mg/Ca ratio because the supersaturation in the bulk solution increased with an increase in CO_3^{2-} concentration. Tai *et al*. [28] and Chien *et al*. [29] revealed the relation between supersaturation in the bulk solution and the rate of crystal nucleation of calcium carbonate in aqueous $CaCl_2$-Na_2CO_3 solution, and the results indicate that the induction period for nucleation decreased with an increase in the supersaturation in the bulk solution. Compared to the previous study, the experimental results obtained in this work indicated that the formation of numerous local regions with a higher supersaturation around the minute gas-liquid interfaces helps the access of Mg/Ca ratio to 1.0 at lower the overall supersaturation in the bulk solution. Additionally, the $CaMg(CO_3)_2$ crystallization in the $CaCO_3$ suspended system at temperatures below 373 K via replacement of the calcite reactant is extremely slow and proceeds

E-mail address: matsumoto.masakazu@nihon-u.ac.jp Phone: +81-47-474-2850

through the intermediate disordered phases according to Usdowski [6,7]. For the production of $CaMg(CO_3)_2$ with a Mg/Ca ratio of 0.9 - 1.0 at a reaction temperature of 296 K the reaction time of 96 hours and high Ca^{2+} and Mg^{2+} ion concentrations are consequential, as suggested by Oomori *et al*. [21]. Compared to the previous research, the formation of numerous local regions with a higher supersaturation around the minute gas-liquid interfaces caused by increase in F_{CO2} during reactive crystallization with CO_2 microbubble injection remarkably decreased the reaction time for the achievement of a higher Mg/Ca ratio.

3.3 Relationship between CO_2 flow rate and Mg/Ca ratio or induction time for nucleation

From the above results obtained by varying d_{bbl}, F_{CO2}, the nucleation rate (r_{nuc}) was determined from the reciprocal of the induction period for nucleation, and the rate of increase in the Mg/Ca ratio ($r_{Mg/Ca}$) was calculated from the initial gradient of the time change in the Mg/Ca ratio. The relationship between r_{nuc} and $r_{Mg/Ca}$ is shown in **Fig. 5**.

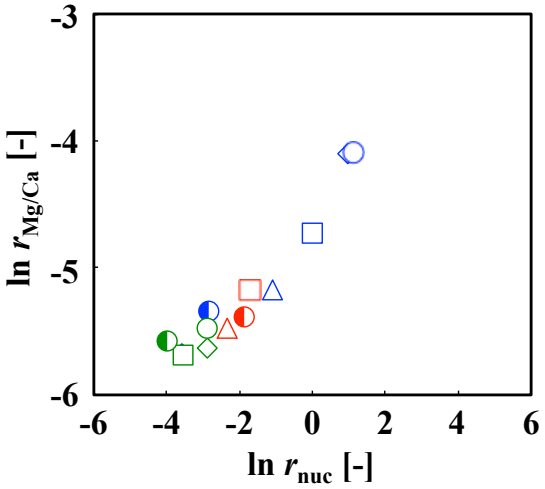

F_{CO2} [mM/min]	d_{bbl} [μm] 40	300	2000
1.49	▽		
2.58	◐		
5.96	△	▲	
8.93		◐	◐
11.9	□	□	□
17.8	◇		◇
23.8	○		○

Fig.5 Relationship between r_{nuc} and $r_{Mg/Ca}$

Under the experimental conditions investigated in this work, a positive correlation was observed between r_{nuc} and $r_{Mg/Ca}$. In general, the increasing supersaturation in the bulk solution leads to the generation of $CaMg(CO_3)_2$ with high Mg/Ca ratio. Kotaki and Tsuge evaluated the nucleation of calcium carbonate in a gas-disparger tank crystallizer, and discussed the relation between supersaturation in the bulk solution and crystal nucleation from the particle size of the calcium carbonate produced [30]. As a result, in a gas-liquid-solid system where the gas is dispersed as bubbles, the higher supersaturation is localized in the area surrounding the gas-liquid interfaces in the liquid phase. Thus, crystal nucleation is accelerated in the regions with the higher supersaturation. On the other hand, in a liquid-liquid-solid system, the supersaturation in the bulk solution is nearly uniform, so that the particle growth proceeds predominantly compared to the crystal nucleation. Therefore, microbubble injection that enables the acceleration of crystal nucleation owing to a local increase in the supersaturation at the minute gas-liquid interfaces caused by the electric charge on the microbubble surface and the acceleration of the CO_2 mass transfer is effective for the high-yield crystallization of $CaMg(CO_3)_2$ fine particles with the Mg/Ca ratio of 1.0.

E-mail address: matsumoto.masakazu@nihon-u.ac.jp Phone: +81-47-474-2850

[1] Nihon University, [2] Research Institute of Salt and Sea Water Science, [3] Chiba Institute of Technology
M. Matsumoto[1*], K. Masaoka[2], Y. Tsuchiya[1], Y. Wada[1], T. Hiaki[1], K. Onoe[3]

Conclusions

The reactive crystallization of $CaMg(CO_3)_2$ by CO_2 microbubble injection from the concentrated brine at a reaction temperature of 298 K was performed by various d_{bbl} and F_{CO2} values to produce $CaMg(CO_3)_2$ fine-particles with the Mg/Ca ratio of 1.0. This investigation revealed the following; 1) at a constant F_{CO2} of 11.9 mmol/(l·min), the minimization of the bubble diameter led to the linear increase in $W_{dolomite}$ and Mg/Ca ratio and the micronization of $CaMg(CO_3)_2$ because of the acceleration of CO_2 absorption and the electrification of the microbubble surface; 2) when F_{CO2} was increased to 23.8 mmol/(l·min) during reactive crystallization supplying CO_2 microbubbles with a d_{bbl} of 40 μm, the Mg/Ca ratio reached 1.0; and 3) under the experimental conditions employed in this study, a positive correlation was observed between r_{nuc} and $r_{Mg/Ca}$.

Acknowledgements

This work was financially supported by the Salt Science Research Foundation (No.1523, No.1620), Japan. We also acknowledge the Naikai Salt Industry Co., Ltd. for provision of Bittern.

References

[1] M. Matsumoto, Y. Wada, K. Onoe, Bulletin of the Society of Sea Water Science, Japan 69 (2015) 262, in Japanese.

[2] M. Matsumoto, Y. Wada, K. Onoe, Bulletin of the Society of Sea Water Science, Japan 68 (2014) 323, in Japanese.

[3] E. Alvarado, L.M. Torres-Martinez, A.F. Fuentes, P. Quintana, Polyhedron 19 (2000) 2345.

[4] A.N. Copp, American Ceramic Society Bulletin, 75 (1996) 135.

[5] G. Li, Z. Li and H. Ma, Appl. Clay Sci., 86 (2013) 145.

[6] E. Usdowski, Naturwissenchaften, 76 (1989) 374.

[7] E. Usdowski, “Synthesis of dolomite and geochemical implications”, in: M.E. Tucker and D. Zenger (Eds.), Special Publication Number 21 of the International Association of Sedimentologists, Oxford (1994) 345.

[8] R.V. Lloyd, C.S. Morie, D.N. Lumsden, Chemical Geology 105 (1993) 253.

[9] S.H.Hordeng, D.F.Sibley Geochimica et Cosmochimica Acta 58 (1994) 191.

[10] K.Sato, T.Katsura, Earth and Planetary Science Letters 184 (2001) 529.

[11] D.M. Burt, H.D. Holland, Geochimica et Cosmochimica Acta 41 (1977) 297.

[12] A. Karz, A. Matthews, Geochimica et Cosmochimica Acta 31 (1967) 391.

[13] D.N. Lumsden, Lisa G Shipe, Roger V Lloyd, Geochimica et Cosmochimica Acta 53 (1989) 2325.

[14] M. Maunaye, H. Anoun, M.L. Guyader, Comptes Rendus de Academie des Science Series 2 paris, 293 (1981) 753.

E-mail address: matsumoto.masakazu@nihon-u.ac.jp Phone: +81-47-474-2850

[15] T. Oomori, K. Kaneshima, T. Taira, Y. Kitano, Geochemical journal 17 (1983) 147.

[16] M. Matsumoto, Y. Morita, M. Yoshinaga, S. Hirose, K. Onoe, Journal of Chemcal Engineering Japan 42 (2009) s242.

[17] M. Matsumoto, T. Fukunaga, K. Onoe, Journal of Chemical Engineering Research and Design 88 (2010) 1624.

[18] Y. Wada, M. Matsumoto and K. Onoe, J. Cryst. Growth, 373 (2013) 92.

[19] Y. Tsuchiya, Y. Wada, K. Masaoka, M. Okada, T. Sato, T. Hiaki, K. Onoe, M. Matsumoto, Bulletin of the Society of Sea Water Science, Japan 71 (2017) 103.

[20] Y. Tsuchiya, Y. Wada, T. Hiaki, K. Onoe, M. Matsumoto, Journal of Crystal Growth 469 (2016) 36.

[21] T. Oomori, K. Kaneshima, T. Taira and Y. Kitano, Geochemistry Journal 17 (1983) 147.

[22] H. Mitsusio, H. Nishizawa, K. Matsuoka, Research Report of Kochi University Natural science 32 (1983) 327, in Japanese.

[23] T. Oomiri, Y. Kitano, Geochemical journal 21 (1987) 59.

[24] Goldsmith, J. R., and D. L. Graf, American Mineralogist 43 (1958) 84.

[25] Goldsmith, J. R., and O. I. Joensuu, Geochimica et Cosmochimica Acta 7 (1955) 212.

[26] Kubota, N., T. Sekimoto and K. Shimizu, Journal of Crystal Growth 102 (1990) 434.

[27] H. Fujimura, T. Oomori, S. Kochi, T.A. Prolla, S. Someya, Food chemistry 99 (2006) 15.

[28] C.Y. Tai, W.C. Chien, Journal of Crystal Growth 237 (2002) 2142.

[29] W.C. Chein, C.C. Lee, C.Y. Tai, Industrial & Engineering Chemistry Research 46 (2007) 6435.

[30] Kotaki, Y. and H. Tsuge, Canadian Journal of Chemical Engineering 68 (1990) 435.

E-mail address: matsumoto.masakazu@nihon-u.ac.jp Phone: +81-47-474-2850